

Beam Pull Out Tests of NSM – FRP and Steel Bars in Concrete

D. G. Novidis and S. J. Pantazopoulou

Department of Civil Engineering, Demokritus University of Thrace

Phone: +3025410-79639, address: Vas. Sofias #12A, Xanthi 67100, Greece

Emails: dnovidis@civil.duth.gr, pantaz@civil.duth.gr

ABSTRACT: This paper describes an experimental investigation regarding a relatively new strengthening method for flexural concrete members, known as NSM technology (near-surface mounting). The study included fourteen simply supported concrete beams, strengthened by placing either steel or carbon FRP bars in grooves cut on the tension face of the member and bonding with epoxy paste; specimens were loaded in bending till the occurrence of failure by debonding. Nine of the specimens were fabricated to have the bar fully bonded in one half-span, whereas the bonded length in the other half span of the typical member was limited. The bonded length was a parameter of study in the investigation. NSM bars were fully bonded in the case of the remaining five specimens. An objective of this experimental research was to examine the bond strength of the NSM method using realistic stress field conditions (beam pullout tests rather than standard pullout) while at the same time obtaining test results for comparison with those of the direct pull out tests. From the experimental evidence it is concluded that flexural curvature, which occurs in the beam-type tests, has a significant effect on the mode of failure of the upgraded system and on the strength of the failure interface, with a magnitude that depends strongly on the mechanical properties and the surface pattern of the bar. With increasing height of the surface deformations of smooth bars, the failure mode gradually changes from pullout at the bar-epoxy interface, to failure at the epoxy-concrete interface which is also observed in standard pullout tests. In this case, bond strength obtained from the beam tests is in general greater than the respective value recorded from direct pull out tests. This increase is attributed to the additional friction generated on the bar and on the epoxy filler's lateral surface owing to curvature compatibility between the bar and the surrounding concrete in the bending beam.

1 INTRODUCTION

The NSM strengthening method has gained renewed interest recently, with the advent of advanced composite materials which made solutions possible for strength increase without the susceptibility to corrosion, in reinforced concrete structures with diagnosed flexural strength deficiencies (e.g. slabs or beams with corroded primary reinforcement, increase of design loads etc). This option was explored as an alternative to the well known EBR (Externally Bonded Reinforcement) technique, whereby strength and failure are almost always limited by premature debonding in the ends of the attached reinforcement owing to the low tensile strength of the concrete cover (Oehlers & Moran 1990, Malek et al. 1998, De Lorenzis & Nanni 2001 and Novidis & Pantazopoulou 2007,a). Once placed in longitudinal surface grooves (cut in the cover of the member that requires strengthening) and surrounded by the hardened epoxy filler, the bars are subjected to compatible displacement conditions with the surrounding concrete, as occurs with the existing embedded reinforcement. Because they are generally located outside the embedded stirrups (in actual concrete members of a structure), bond and development capacity of the NSM bars are critical parameters in determining their effectiveness as added primary rein-

forcement and in securing composite action with the existing member. Bond also determines the strength and the eventual failure mode of the upgraded member. In this regard, bond strength is controlled entirely by the surface characteristics and bar stiffness, the groove dimensions and the shear behaviour of the filler material (usually epoxy paste). Stress transfer and interaction occurs along the two contact surfaces: (a) at the interface between bar and epoxy and (b) at the interface between the epoxy and the surrounding concrete. In both cases, force transfer is achieved through chemical adhesion at the early stages and through friction for higher levels of slip. Mechanical interlocking between bar and epoxy may occur if the bar used has surface deformations. Usually the failure occurs at one of the two contact interfaces: Pullout tests in controlled laboratory conditions usually are marked by failure at the concrete – epoxy surface (Novidis & Pantazopoulou 2006), although failures by splitting have also been reported if a cementitious mortar is used instead of epoxy paste as a filler material. In different setups such as in beam tests bar pullout has also been reported (failure at the bar-epoxy paste interface and epoxy splitting, Novidis and Pantazopoulou 2006). The ductility of the failure mode depends entirely on the properties of the system. If the filler material is epoxy paste, (most often an elastic brittle material with a high tensile resistance), precipitous debonding is expected to occur in either of the two contact surfaces without stress redistribution. In the present paper, parameters of study were the material and surface pattern of the bar, the embedment length, the effect of the specimen type and test setup used (i.e., beam pull out tests as opposed to direct pull out tests) and finally the shear-span and the crack pattern of the beams. Test results are used to indicate the effect of investigated parameters on bond strength in order to support drafting of practical design recommendations for strengthening applications of reinforced concrete members with post-installed near-surface mounted reinforcement.

2 EXPERIMENTAL DATA OF THE STUDY

The experimental study comprised a total of 14 simply supported unreinforced concrete beams, tested under three-point load (Figure 1a). Cylindrical seats were used as supports at the beam ends. Quasi-static load was applied at mid-span using a 200.0 kN piston, and was increased monotonically to specimen failure.

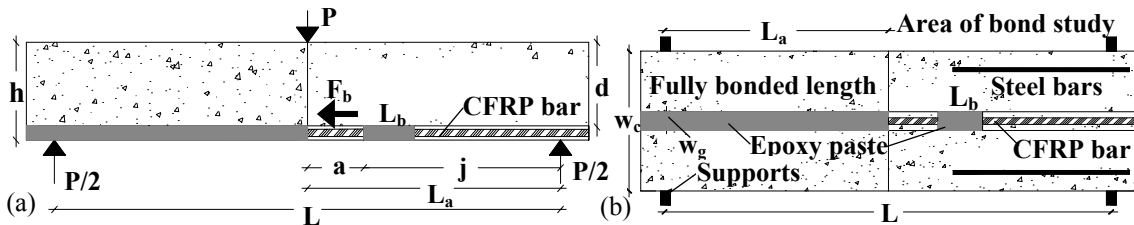


Figure 1. Geometrical characteristics of beam specimens: (a) side view and (b) plan view.

All beams had a rectangular cross-section 150.0 mm high by 300.0 mm wide. Beams were classified in ten specimen cases (S.C.) according with the values of the parameters studied. Cases 9 and 10 concern beams 2000.0 mm long, having a span to depth ratio, $L_a/h=6$ (hereby referred to as aspect ratio). All other cases considered were 1000.0 mm long with an aspect ratio of 3. Surface grooves having a 20mm square cross section were preformed and the NSM bars were post-installed after normal curing (28 days) using an epoxy paste. In all specimens, the surface of the grooves was artificially roughened using a metallic brush to improve adhesion of the epoxy paste-concrete interface through interlocking. To achieve uniform stress distribution over the anchorage so as to reliably quantify the local bond strength from the tests, short anchorage lengths were used ($5D_b$ and $10D_b$). Commercially supplied C25/30 concrete was used, having an average 28-day compressive strength of 33.50 MPa as determined from standard (ASTM C39) concrete cylinder tests. Nominal CFRP bar properties were as follows (as specified by the manufacturer): modulus of elasticity = 124.0 GPa, ultimate strain at tensile rupture = 1.7%. Bar surface patterns were either sand-coated or sand-blasted.

Table 1. Summarized test results for all beam-specimens, (beams with anchorage length of $5D_b$ and $10D_b$ were tested in replicas of two)

Specimen code	Length L (mm)	Actual D_b (mm)	Filler material	Bonded length L_b (D_b)	a (mm)	j (mm)	Bar material	Surface pattern	$P_u / 2$ (kN)	$\delta_{u,80\%}$ (mm)	F_b (kN)	Slip at failure interface (mm)	f_b^c (MPa)	f_b^b (MPa)	F.M.
1-5D-CF	900	9	Epoxy	5	100	350	CFRP	Sand-coated	8,64	1,70	23,98	0,14	8,88	18,85	1
2-10D-CF	900	9	Epoxy	10	100	350	CFRP	Sand-coated	11,39	2,37	31,63	0,36	5,86	12,43	1
3-10D-CF	900	9	Epoxy	10	100	350	CFRP	Sand-blasted	13,00	2,60	36,11	0,41	6,69	14,19	2
4-10D-SS	900	8	Epoxy	10	100	350	Steel	Smooth	7,25	0,60	20,14	0,15	4,20	10,02	2
*5-FB-CF	900	9	Epoxy	50	-	-	CFRP	Sand-blasted	29,50	7,31	-	-	-	-	1
*6-FB-SS	900	8	Epoxy	56	-	-	Steel	Smooth	7,50	12,60	-	-	-	-	3
**7-EM-CF	900	9	-	50	-	-	CFRP	Sand-blasted	23,25	5,17	-	-	-	-	4
*8-FB-SD	900	8	Epoxy	56	-	-	Steel	Deformed	11,25	23,45	-	-	-	-	3
9-10D-CF	1900	9	Epoxy	10	600	350	CFRP	Sand-blasted	8,13	5,39	29,02	0,33	5,38	11,40	2
*10-FB-CF	1900	9	Epoxy	106	-	-	CFRP	Sand-blasted	27,75	19,10	-	-	-	-	5

* FB = Fully Bonded bar with epoxy paste; ** EM = Embedded bar in the concrete; F.M. = Failure Modes: 1 = failure at the epoxy-concrete interface; 2 = failure by pullout at the bar-epoxy interface; 3 = steel fracture; 4 = slipping of the bar into the concrete body of the beam and 5 = splitting of concrete-epoxy cover of the bar followed by slipping bar into the epoxy. (f_b^c and f_b^b are average bond strengths for epoxy-concrete interface and for bar-epoxy interface respectively). $\delta_{u,80\%}$ is the midspan deflection in the post-peak branch corresponding to a residual strength equal to 80% of the peak value.

Table 2. Summarized test results of load-deflection for beams 5,6,7,8 and 10 (evolution of crack pattern)

Specimen code	1 st crack		2 st crack		3 st crack		4 st crack		Values of stable crack pattern		Failure	
	* $P'_{cr,1}$	** $\delta_{cr,1}$	$P'_{cr,2}$	$\delta_{cr,2}$	$P'_{cr,3}$	$\delta_{cr,3}$	$P'_{cr,4}$	$\delta_{cr,4}$	$P'_{cr,s}$	$\delta_{cr,s}$	$P_u / 2$	δ_u
5-FB-CF	9,50	0,72	15,30	2,50	18,15	4,24	-	-	18,15	4,24	29,50	11,70
6-FB-SS	6,25	0,73	-	-	-	-	-	-	6,25	0,73	7,50	0,92
7-EM-CF	7,00	0,24	14,50	2,40	18,25	4,87	-	-	18,25	4,87	23,25	8,41
8-FB-SD	9,50	0,10	10,75	0,58	-	-	-	-	10,75	0,58	11,25	8,76
10-FB-CF	5,75	0,83	8,25	2,43	12,00	6,34	15,75	10,84	15,75	10,84	27,75	28,60

* = Units (kN) and $P'_{cr,i} = P_{cr,i} / 2$; ** = Units (mm).

Epoxy paste was prepared by mixing the two components (resin and hardener) and the mechanical properties, as specified by the manufacturer (ASTM D790), were a tensile strength of 30.0 MPa and a modulus of elasticity of 3.0 GPa. From previous splitting tests the tensile strength of the epoxy paste was found to be 22.6 MPa. When used as NSM inserts, steel bars were smooth except for one case where deformed S500 bars were used, having a modulus of elasticity of 210.0 GPa. Geometric characteristics together with test results for all beam specimens are summarized in Figure 1 and Tables 1 and 2 respectively. Mid-span displacement was measured using a linear-variable differential transducer (LVDT) at midspan. Slip of the bar and epoxy relative to the concrete beam was recorded through strain gauges at the “loaded end” and at the “free end” of the anchored bar-epoxy system.

3 PRESENTATION AND EVALUATION OF TEST RESULTS

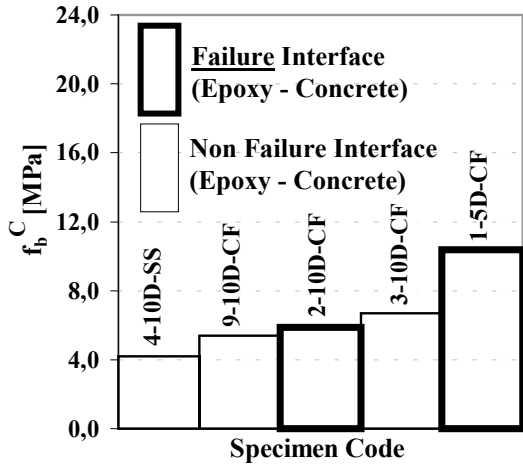


Figure 2. Average bond strength (f_b^c) for all bond specimens.

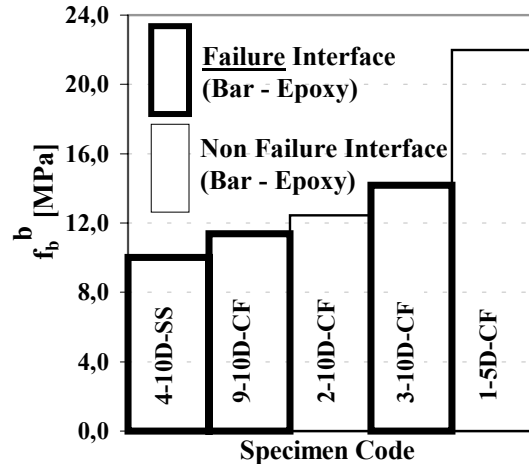


Figure 3. Average bond strength (f_b^b) for all bond specimens.

Figures 2 - 6 outline the experimental results highlighting the effect of the experimental study parameters on average bond strength obtained for the group of bond specimens that had a bonded NSM-bar length of $5D_b$ and $10D_b$. To avoid concrete tension failure, these specimens were reinforced with two short-length deformed steel bars in the area of study, as illustrated in Figure 1(b). Two alternative failure modes were observed throughout the bond tests, as depicted in Figures 2 and 3; thus, for specimens where the surface pattern of the bar was sand-coated (S.C.: 1 and 2), failure occurred by sliding along the epoxy-concrete interface whereas for specimens having sand-blasted or smooth bars failure occurred at the other contact surface, (at the bar-epoxy interface, S.C.:3, 4 and 9).

Test results from a previous experimental study on bond of NSM bars conducted on modified direct pullout prismatic specimens with the same groove and material characteristics as those used in the present investigation showed failure at the epoxy-concrete interface even for sand-blasted bars (Novidis & Pantazopoulou 2006). This difference in the mode of failure effected by the specimen type (beam test used here, versus modified direct pullout in the former study) is confirmed also by other beam tests. The authors attribute this difference in behaviour to the flexural curvature occurring in beam tests during loading. Note that the deflected shape of the bar, $w_b(x)$, is prescribed by that of the deflecting beam owing to compatibility requirements. This form is equivalent to the existence of a nontrivial normal pressure, $q_b(x)$, acting normal to the bar surface, through the relationship:

$$\frac{d^4 w_b(x)}{dx^4} = \frac{q_b(x)}{EI_b} \quad (1)$$

This general relationship holds for any type of bar material; considering that the stiffness of the

composite bars studied in the present study is approximately half the value of that of steel reinforcement ($124\text{GPa}/210\text{GPa}=0.59$) it is evident that under the same external load, deflections and curvature will be doubled in the case of the CFRP-reinforced beams as compared to steel-reinforced beams of equal reinforcing area. The change in the trajectory of the bar axial force as it follows the deflections of the beam generates a distributed normal pressure approximately equal to $P \cdot \tan(\alpha) \approx P \cdot \alpha$, where P is the bar force and α the curvature (i.e., $\alpha = d^2 w_b / dx^2$). For usual cases and normal levels of deflection this pressure is found to be significant. This pressure acting normal to the lateral surface of the NSM-bar encourages the development of friction and thereby mechanical interlock at both interfaces thereby enhancing the system's resistance. From basic mechanics it may be shown that the estimated distributed friction along the length of the contact surface, τ_{curv} , which is to be added to other conventional sources of bond, and is owing solely to the presence of curvature, equals:

$$\tau_{\text{curv}} = \mu \cdot P \cdot \alpha \quad (2)$$

For example: a 12mm GFRP bar, with cross section area, $A=112\text{mm}^2$, functioning at a stress of 300MPa, the bar strain is, 0.0024, and the corresponding curvature, $\alpha=0.0024/(0.6 \cdot d)=3 \times 10^{-5}$, where d the effective depth of the cross section, here taken as $d=130\text{mm}$. Therefore, $\tau_{\text{curv}}=300 \times 112 \times (3 \times 10^{-5})=1.0 \text{ N/mm}=1.0\text{kN/m}$.

Considering the results of this study, it is clear that the described influence of radial pressure on the prevailing failure mode (concerning the weakest interface) has been seen in cases of specimens strengthened with the NSM procedure using either smooth bars or slightly deformed bars, such as would be the surface of a sand-blasted bar. A limit to the height of surface deformation of the bar has to be considered, as this phenomena (effect of specimen form on failure mode) appears to be suppressed when the surface roughness is substantial (e.g. specimens with sand-coated bars having grains of sand, 0.5-1.0 mm high). Thus, beyond this height limit on bar deformations the cohesion between epoxy-concrete surfaces becomes the weak link regardless of specimen form or test setup.

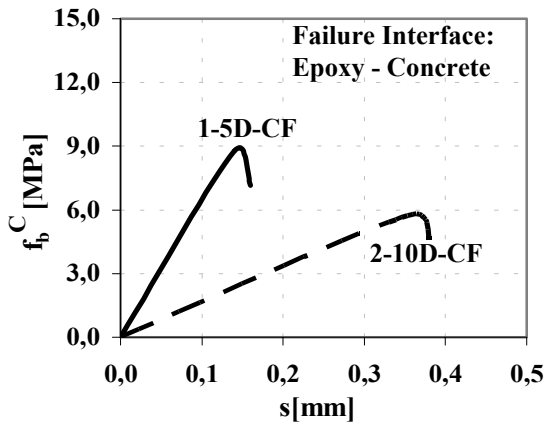


Figure 4. Average bond strength (f_b^c) vs. slip for different anchorage lengths.

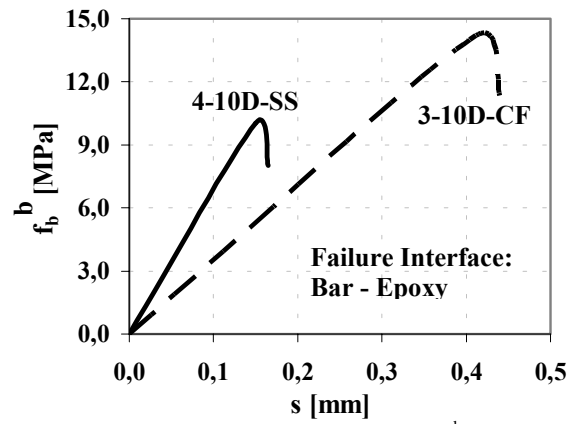


Figure 5. Average bond strength (f_b^b) vs. slip for different bar materials.

Figure 4 depicts the effect of different bonded lengths on average bond strength. As the bonded length increases the development capacity as quantified by the total load carried by the joint increases. However, the average bond strength decreases due to the non-uniform distribution of bond stresses. This reduction of average bond strength was observed when the available bonded length exceeded the limit value of $5D_b$, (Novidis et al. 2007). Average bond strength reduction was observed also when using steel smooth bar inserts (greater bar stiffness) as compared with CFRP sand-blasted bar inserts, Figure 5, (Novidis & Pantazopoulou 2007,b). As both steel and CFRP bars used were smooth with insignificant surface roughness (sand-blasted), mechanical interlock between bars and epoxy was limited to the wedging action. Initial chemical

adhesion appears to be stronger in the case of the CFRP bars at the contact surface with the epoxy, rather than in the case of smooth steel bars. Another reduction in bond strength was also observed when doubling the span length of the beam specimens, (Fig. 6). This result is attributed to the higher amount of slip (quantified by crack widths) in the shear span owing to the larger amounts of deflection, leading to an earlier failure of the beam by bar pull out from the epoxy paste. Specimens with steel bars (S.C. 6 and 8, fully bonded) failed by bar rupture after bar yield, at relative small load and high plastification in comparison with the respective specimens with CFRP bars (S.C. 5 and 10), since the shear strengths at the two contact surfaces (epoxy-concrete and steel bar-epoxy) were shown to be considerably higher than the tensile strength of the steel bars, (Figs 7, 8).

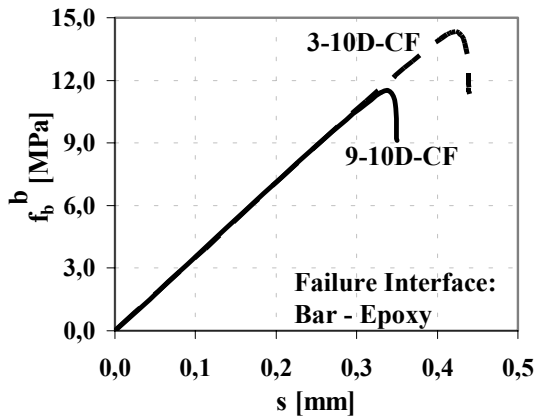


Figure 6. Average bond strength (f_b^c) vs. slip for different spans.

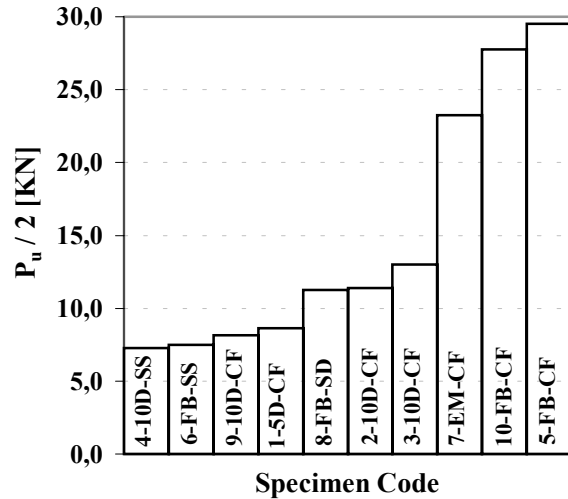


Figure 7. Ultimate load for all specimens.

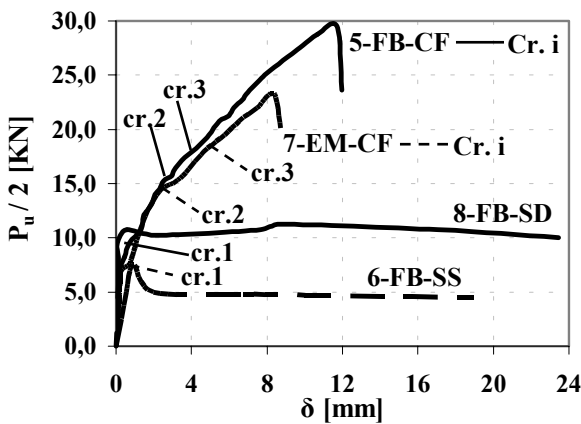


Figure 8. Crack propagation during loading for specimens with different bar materials and bar embedment method.

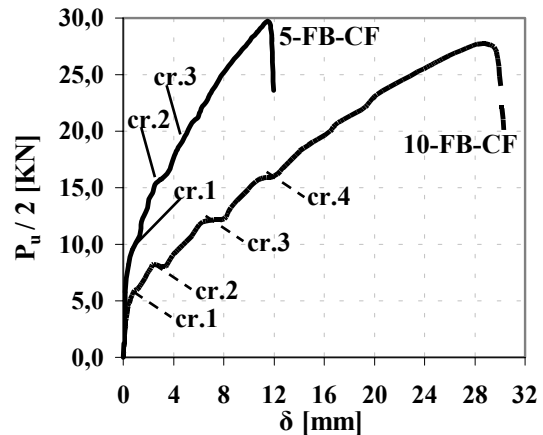


Figure 9. Crack propagation during loading for specimens with different spans.

Results for the two fully bonded specimens are shown in Figure 8. In the first of those the FRP bar had been embodied in the concrete during casting of the beam (S.C. 7) whereas in the second the FRP bar was post-installed in the groove through epoxy paste (S.C. 5). Both specimens were close in all aspects (crack propagation and stiffness) except for the final strength of the beam, which was 25% higher in the latter case with the epoxy paste (Fig. 8). This result highlights the improved chemical adhesion and friction between CFRP bar and the epoxy as compared with the magnitude of adhesion at the contact between CFRP bar and concrete. Higher plastification was observed in specimens with steel bars in contrast with specimens reinforced with CFRP bars; this was as expected owing to the different stress-strain characteristics

of the two materials (brittleness of the FRP bars). Crack propagation was more intense in specimens with CFRP bars (Fig. 8), as well as in cases with longer span lengths (specimen 10-FB-CF, Fig. 9). Crack spacing was almost doubled in the latter case as compared with the corresponding specimens having CFRP bars and an aspect ratio of 3. (Note that recorded crack spacing after crack stabilization was in the range of 100 to 150 mm for S.C. 5 and 7, and up to a value of 250 mm for S.C. 10).

4 CONCLUSIONS

Bond behaviour of NSM-FRP bars was studied experimentally through testing of simply supported beam-specimens, after strengthening the beams with this technology. Parameters of study were the bar stiffness (steel vs. CFRP), surface roughness (sand blasted vs. bars with helical indentations, steel smooth bars, and steel deformed bars), and manner of bar placement (post-installed in surface grooves, or embedded during initial casting). An additional parameter was beam span length so as to provide data and insight regarding the influence of beam curvature on measured bond strength. The primary finding of the study is that this technology can mitigate the problems of debonding from the ends, commonly observed when strengthening beams through externally bonded FRP laminates. Beam curvature was found to increase the contact bond strengths at both interfaces moving the occurrence of failure to the weakest interface which however depends on the height of bar surface deformation; this represents a significant deviation from results obtained when the embedded bar is pulled on its axis without eccentricity. Further investigations of this problem are under development.

5 ACKNOWLEDGEMENTS

This investigation was conducted in the Laboratories of the Department of Civil Engineering, Democritus University of Thrace (DUTH), Xanthi - Greece under a research program funded by the Hellenic General Secretariat for Research and Technology (PENED2001). MAC BETON HELLAS S.A. generously donated the epoxy-pastes used in the experimental program. FRP reinforcement was purchased from Hughes Brothers (USA).

6 REFERENCES

- De Lorenzis L. and Nanni A. (2001). "Characterization of FRP Rods as Near-Surface Mounted Reinforcement", *ASCE J. of Composites for Construction*, Vol. 5, No. 2, pp.114-121.
- Malek AM., Saadatmanesh H. and Ehsani MR. (1998). "Prediction of Failure Load of R/C Beams Strengthened with FRP Plate due to Stress Concentration at the Plate End", *ACI Structural J.*, Vol. 95, No. 1, pp.142-152.
- Novidis, D. G. and Pantazopoulou, S. J. (2006). "Experimental Study of Short NSM – FRP & Steel Bar Anchorages", *Proceedings of the 2nd Int. of fib Congress, Naples, Italy*.
- Novidis D. G., Pantazopoulou S. J. and Tentolouris E. (2007). "Experimental Study of Bond of NSM – FRP Reinforcement." *Elsevier, J. of Construction and Building Materials*, Vol. 21, No. 8, pp.1760-1770.
- Novidis D. G. and Pantazopoulou S. J. (2007,b) "Bond Tests of Short NSM – FRP & Steel Bar Anchorages", accepted for publication *ASCE, Journal of Composites for Construction*.
- Novidis D. G. and Pantazopoulou, S. J. (2007,a). "Beam Tests of NSM - FRP Laminates in Concrete", *Proceedings of the 8th Int. Symposium on Fiber Reinforced Polymer Reinforcement for Concrete Structures, FRPRCS-8, Patras, Greece*.
- Oehlers DJ. and Moran JP. (1990). "Premature Failure of Externally Plated Reinforced Concrete Beams", *ASCE J. of Structural Engineering*, Vol. 116, No. 4, pp.978-995.